

RESEARCH

Open Access



The *adc1* knockout with *proC* overexpression in *Synechocystis* sp. PCC 6803 induces a diversion of acetyl-CoA to produce more polyhydroxybutyrate

Suthira Utharn^{1,2} and Saowarath Jantaro^{1*}

Abstract

Background Lack of nutrients, in particular nitrogen and phosphorus, has been known in the field to sense glutamate production via 2-oxoglutarate and subsequently accelerate carbon storage, including glycogen and polyhydroxybutyrate (PHB), in cyanobacteria, but a few studies have focused on arginine catabolism. In this study, we first time demonstrated that gene manipulation on *proC* and *adc1*, related to proline and polyamine syntheses in arginine catabolism, had a significant impact on enhanced PHB production during late growth phase and nutrient-modified conditions. We constructed *Synechocystis* sp. PCC 6803 with an overexpressing *proC* gene, encoding Δ^1 pyrroline-5-carboxylate reductase in proline production, and *adc1* disruption resulted in lower polyamine synthesis.

Results Three engineered *Synechocystis* sp. PCC 6803 strains, including a *ProC*-overexpressing strain (OXP), *adc1* mutant, and an OXP strain lacking the *adc1* gene (OXP/ Δ *adc1*), certainly increased the PHB accumulation under nitrogen and phosphorus deficiency. The possible advantages of single *proC* overexpression include improved PHB and glycogen storage in late phase of growth and long-term stress situations. However, on day 7 of treatment, the synergistic impact created by OXP/ Δ *adc1* increased PHB synthesis by approximately 48.9% of dry cell weight, resulting in a shorter response to nutrient stress than the OXP strain. Notably, changes in proline and glutamate contents in engineered strains, in particular OXP and OXP/ Δ *adc1*, not only partially balanced the intracellular C/N metabolism but also helped cells acclimate under nitrogen (N) and phosphorus (P) stress with higher chlorophyll *a* content in comparison with wild-type control.

Conclusions In *Synechocystis* sp. PCC 6803, overexpression of *proC* resulted in a striking signal to PHB and glycogen accumulation after prolonged nutrient deprivation. When combined with the *adc1* disruption, there was a notable increase in PHB production, particularly in situations where there was a strong C supply and a lack of N and P.

Keywords PHB, *Synechocystis* sp. PCC 6803, Proline, Glycogen, Glutamate

*Correspondence:

Saowarath Jantaro
saowarath.j@chula.ac.th

¹ Laboratory of Cyanobacterial Biotechnology, Department of Biochemistry, Faculty of Science, Chulalongkorn University, Bangkok 10330, Thailand

² Program of Biotechnology, Faculty of Science, Chulalongkorn University, Bangkok 10330, Thailand

Introduction

The cumulative harm caused by pollution and inadequate resource and land management of our remaining natural resources is a major connected element of many global concerns. Microalgae, including cyanobacteria, have the ability to address some of these issues by decreasing aquatic pollutants and offering a sustainable supply of biomass for product development, as evidenced by the



© The Author(s) 2024. **Open Access** This article is licensed under a Creative Commons Attribution 4.0 International License, which permits use, sharing, adaptation, distribution and reproduction in any medium or format, as long as you give appropriate credit to the original author(s) and the source, provide a link to the Creative Commons licence, and indicate if changes were made. The images or other third party material in this article are included in the article's Creative Commons licence, unless indicated otherwise in a credit line to the material. If material is not included in the article's Creative Commons licence and your intended use is not permitted by statutory regulation or exceeds the permitted use, you will need to obtain permission directly from the copyright holder. To view a copy of this licence, visit <http://creativecommons.org/licenses/by/4.0/>. The Creative Commons Public Domain Dedication waiver (<http://creativecommons.org/publicdomain/zero/1.0/>) applies to the data made available in this article, unless otherwise stated in a credit line to the data.

emerging uses of microalgal biotechnology assisting the United Nations' Sustainable Development Goals (SDGs) [1, 2]. The microalgal biomass possesses a wide variety of primary and secondary metabolites that are increasingly being acknowledged for their importance in the production of novel products and biotechnological applications. These valuable products, which can be produced directly from CO₂ via photosynthesis, include pigments such as carotenoids, and chlorophylls, carbon storages such as glycogen and polyhydroxybutyrate (PHB), as well as macromolecular compounds such as proteins, carbohydrates, and lipids [3–9]. There are several strategies for boosting algal biomass in order to achieve the lower carbon restriction that limits the yield of biofuel and bioproducts, including nutritional adjustment, and gene manipulation by genetic and metabolic engineering. The increased CO₂ fixation capacity, such as *RuBisCO* gene overexpression, and glucose utilization, has driven cyanobacteria to have better growth and photosynthesis [6, 10–12], and be able to produce more PHB and lipids [4]. Under nitrogen or phosphorus deficiency, most cyanobacteria preferentially store carbon sources in the forms of glycogen and PHB, which are a consequence of the 2-oxoglutarate balance for carbon/nitrogen control [13–15]. In Fig. 1, the arginine catabolism flux associated with the polyamine synthesis, proline-glutamate reaction, and GS/GOGAT pathway [16, 17]. Previous studies found that a transposon-mutated *Synechocystis* sp. PCC 6803 significantly enhanced PHB synthesis while lacking the *proA* gene encoding gamma-glutamyl phosphate reductase. This mutant also had decreased proline reduction and increased glutamate accumulation [18]. Furthermore, the arginine–ornithine to proline–glutamate reaction was primarily driven by the deletion of the *adc1* gene, which encodes arginine decarboxylase involved in polyamine biosynthesis, in *Synechocystis* sp. PCC 6803. This undoubtedly boosted PHB production, although the precise mechanism is still unknown [5]. Notably, in *Synechocystis* sp. PCC 6803, during nitrogen shortage, the activation of an OmpR-type response regulator (Rre37) may stimulate the metabolic flux from glycogen to PHB as well as the hybrid TCA cycle and arginine–ornithine cycle [9]. In cyanobacteria, glutamate can be synthesized through two alternative systems including GS/GOGAT pathway, and another catalyzed by glutamate dehydrogenase (GDH) [19, 20]. The GS/GOGAT pathway is the main ammonium assimilation system in *Synechocystis* 6803, while GDH encoded by the *gdhA* gene is regulated by the late stage of growth [21, 22] and when energy supply is limited in *Escherichia coli* [23]. On the other hand, when acetyl-CoA flow is driven to PHB accumulation, it is mostly directed to the TCA cycle and fatty acid synthesis from pyruvate and acetate, except for

nutritional constraints (Fig. 1). Enzymes which involved in PHB biosynthesis are β -ketothiolase (*phaA*), acetoacetyl-CoA reductase (*phaB*), and heterodimeric PHB synthase (*phaE* and *phaC*), respectively [24]. Instead of producing new CO₂ fixation, the cyanobacteria that were starved of nutrients favored producing PHB from internally stored carbon storage, such as glycogen [8, 25]. In this study, to supply more glutamate to TCA cycle, we overexpressed the *proC* gene, encoding Δ^1 pyrroline-5-carboxylate reductase (Fig. 1), in *Synechocystis* sp. PCC6803 wild type and Δ *adc1* mutant strains. Two engineered strains included a *Synechocystis* sp. PCC6803 overexpressing *proC* gene or OXP, and *Synechocystis* sp. PCC6803 overexpressing *proC* gene with a knockout of *adc1* gene in polyamine synthesis or OXP/ Δ *adc1* strains. Both engineered strains certainly accumulated higher PHB content, particularly in a nitrogen and phosphorus-deprived BG₁₁ medium with acetate supplementation (BG₁₁-N-P+A). It is important to highlight that, particularly in the presence of BG₁₁-N-P+A, the acetyl-CoA flow was mainly diverted to the PHB biosynthetic pathway.

Results

Overexpression of native *proC* gene in *Synechocystis* sp.

PCC 6803 wild-type and mutant strains

Initially, we constructed four engineered *Synechocystis* sp. PCC 6803 strains, including wild-type control (WTc), Δ *adc1* mutant control (Δ *adc1c*), OXP, and OXP/ Δ *adc1* by double homologous recombination (Table 1, Fig. 2A). For the WTc and Δ *adc1c* strains, they were created by replacing the *psbA2* gene with a *Cm^R* cassette in the genomes of *Synechocystis* sp. PCC 6803 WT and Δ *adc1* mutant, respectively (Fig. 2A). To create a recombinant plasmid pEERM_*proC* (Table 1), a native *proC* (or *slr0661*) gene fragment with a size of 1.0 kb was ligated between flanking regions of the *psbA2* gene of the pEERM vector and the upstream region of *Cm^R* cassette (Fig. 2A). Next, all overexpressing strains were verified by PCR using specific pairs of primers (Additional file 1: Table S1) for their complete segregation and gene location. To confirm the complete segregation, PCR products with Up_*psbA2*-F and Dw_*psbA2*-R primers confirmed the correct size of 3.2 kb, in OXP and OXP/ Δ *adc1* strains (Fig. 2B.1 and B.2, respectively), while there were 2.3 kb in WT and Δ *adc1* strains, and 2.2 kb in WTc and Δ *adc1c* strains. PCR products with ProC-F and *Cm^R*-R primers confirmed the correct size of 1.9 kb in OXP and OXP/ Δ *adc1* strains (Fig. 2C1 and C2, respectively), compared with no band in WT, WTc, Δ *adc1* and Δ *adc1c* strains. In

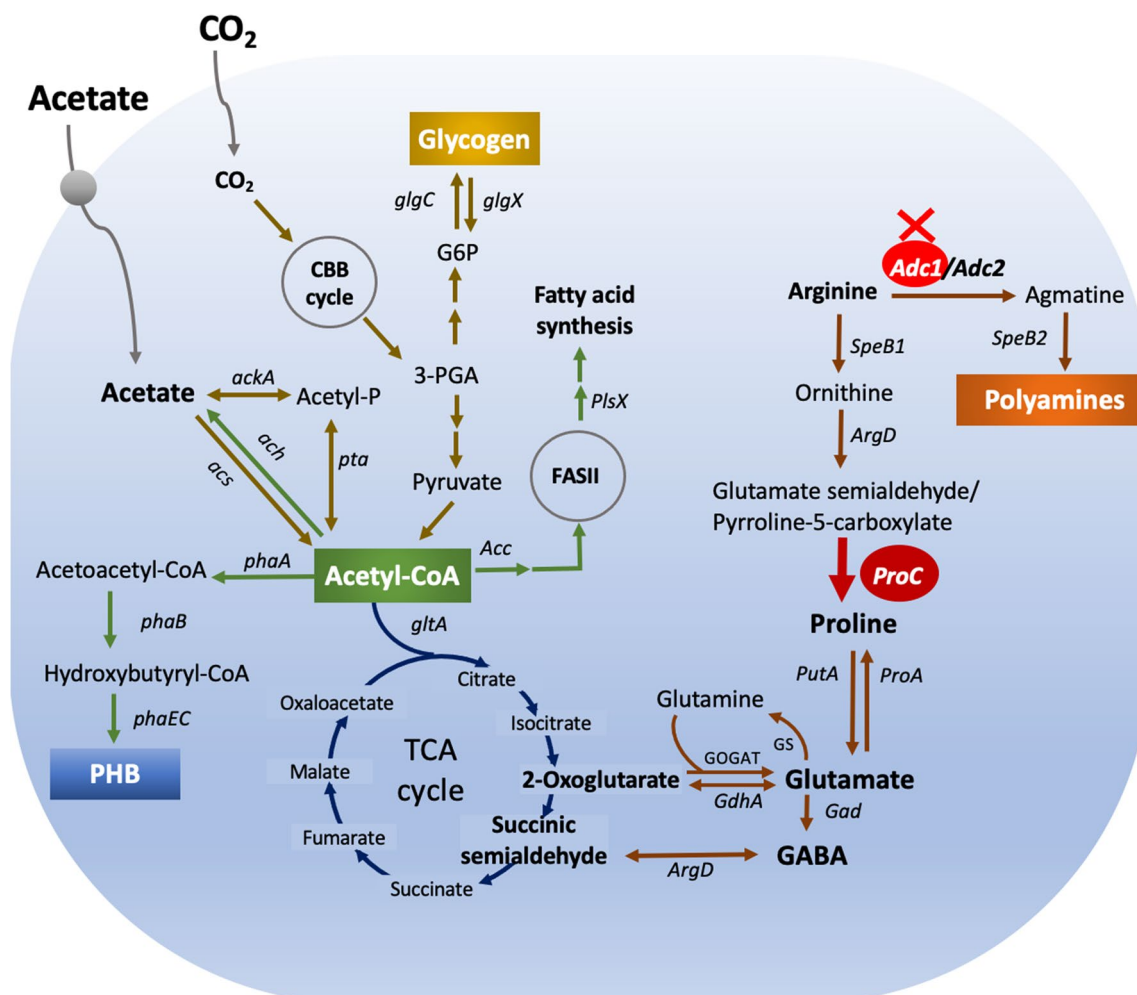


Fig. 1 Overview of the polyamine-proline-glutamate pathways connected to the tricarboxylic acid (TCA) cycle and related biosynthetic pathways of polyhydroxybutyrate (PHB), and glycogen in cyanobacterium *Synechocystis* sp. PCC 6803. Abbreviations of genes are: *acc*, a multisubunit acetyl-CoA carboxylase; *ach*, acetyl-CoA hydrolase; *ackA*, acetate kinase; *acs*, acetyl-CoA synthase; *adc*, arginine decarboxylase; *argD*, N-acetylornithine aminotransferase; *gad*, glutamate decarboxylase; *gdhA*, glutamate dehydrogenase; *glgC*, ADP-glucose pyrophosphorylase; *glgX*, glycogen debranching enzyme; *gltA*, citrate synthase; *plsX*, fatty acid/phospholipid synthesis protein; *phaA*, β -ketothiolase; *phaB*, acetoacetyl-CoA reductase; *phaC* and *phaE*, the heterodimeric PHB synthase; *proA*, gamma-glutamyl phosphate reductase; *proC*, Δ^1 pyrroline-5-carboxylate reductase; *pta*, phosphotransacetylase; *putA*, proline oxidase; *speB1*, arginase; *speB2*, agmatinase. Abbreviations of intermediates are: FASII, fatty acid synthesis type II; GABA, gamma-aminobutyric acid; GOGAT, glutamate synthase; G6P, glucose-6-phosphate; GS, glutamine synthetase; 3-PGA, 3-phosphoglycerate; PHB, polyhydroxybutyrate

addition, *ProC* gene overexpression was verified by RT-PCR data in all engineered strains (Fig. 2D).

Growth, intracellular pigment contents, oxygen evolution rates, and metabolite accumulation under normal growth condition

We found a slight increase in cell growth of the $\Delta adc1c$ and OXP/ $\Delta adc1$ strains in comparison with the WTc and OXP strains (Fig. 3A). All strains had comparable amounts of chlorophyll *a*; however, *proC* overexpression in OXP and OXP/ $\Delta adc1$ had an impact on the

decrease of carotenoids (Fig. 3B, C). In comparison to WTc, all engineered strains showed lower rates of oxygen evolution (Fig. 3D). On the other hand, as anticipated, total polyamines (PAs) in both bound and free forms declined in the $\Delta adc1c$ and OXP/ $\Delta adc1$ strains, but the OXP strain showed a minor decrease in total PAs as compared to the WTc strain (Fig. 3E). It was found that bound PAs were the main decrease when the *adc1* gene was disrupted. On day 7 under normal growth condition, the proline levels of OXP and OXP/ $\Delta adc1$ strains were found to be much higher, but the

Table 1 Strains and plasmids used in this study

Name	Relevant genotype	References
Cyanobacterial strains		
<i>Synechocystis</i> sp. PCC 6803	Wild type	Pasteur culture collection
$\Delta adc1$	$\Delta adc1$ knockout, Km^R inserted between <i>adc1</i> gene in <i>Synechocystis</i> genome	[5]
WT control (WTc)	WT, Cm^R integrated at flanking region of <i>psbA2</i> gene in <i>Synechocystis</i> genome	This study
$\Delta adc1$ control ($\Delta adc1c$)	$\Delta adc1$, Cm^R integrated at flanking region of <i>psbA2</i> gene in <i>Synechocystis</i> genome	This study
OXp	<i>ProC</i> , Cm^R integrated at flanking region of <i>psbA2</i> gene in <i>Synechocystis</i> WT genome	This study
OXp/ $\Delta adc1$	<i>ProC</i> , Cm^R integrated at flanking region of <i>psbA2</i> gene in <i>Synechocystis</i> $\Delta adc1$ genome	This study
Plasmids		
pEERM	P_{psbA2} - Cm^R ; plasmid containing flanking region of <i>psbA2</i> gene	[26]
pEERM_ <i>ProC</i>	P_{psbA2} - <i>ProC</i> - Cm^R ; integrated between <i>SpeI</i> and <i>PstI</i> sites of pEERM	This study

P_{psbA2} , *psbA2* promoter; Cm^R , chloramphenicol resistance cassette

$\Delta adc1c$ strain has the lowest proline content (Fig. 3F). Moreover, the WTc strain exhibited significant glutamate content that was almost ten times greater than proline under normal growth conditions (Fig. 3G). All mutant strains, especially the OXP/ $\Delta adc1$ strain, had a greater increase in glutamate content than the WTc. Similarly, on day 7 of culture, the GABA level in WTc was higher than the proline content but somewhat lower than the glutamate content under normal condition (Fig. 3H). The GABA content of all engineered strains, especially OXP/ $\Delta adc1$, was lower than that of the WTc strain. Glutamate appeared to be the preferred compound that *Synechocystis* cells accumulated, followed by GABA and proline. On the other hand, cells substantially produced a low level of PHB by about 4 – 23% w/DCW under normal growth condition (Fig. 3I). When compared to the WTc, the PHB quantity in the

OXp and OXP/ $\Delta adc1$ strains appeared to be larger. In order to adapt to the nutrient-modified medium, cells growing on day 11, which represents the late-log phase of cell growth with the maximum level of PHB accumulation, were subsequently selected.

Growth, intracellular pigment contents, and metabolite accumulation under nutrient-modified conditions

All *Synechocystis* strains were grown in normal BG₁₁ medium for 11 days before starting the adaptation phase (Fig. 4). Both two nutrient-modified media, including BG₁₁ lacking nitrogen and phosphorus (BG₁₁-N-P) and BG₁₁-N-P medium with acetate addition (BG₁₁-N-P + A), caused a certain reduction in growth (Fig. 4A–C) and intracellular contents of chlorophyll *a* and carotenoids (Fig. 4D–I). It is worth noting that all engineered strains had a slightly higher level of cell growth under the

(See figure on next page.)

Fig. 2 Genomic maps and transcript levels of *Synechocystis* sp. PCC 6803 strains. The four constructed strains are *Synechocystis* sp. PCC 6803 wild-type control (WTc), *Synechocystis* sp. PCC 6803 lacking *adc1* gene ($\Delta adc1c$), *Synechocystis* sp. PCC 6803 overexpressing *proC* gene (OXp), and $\Delta adc1$ mutant overexpressing *proC* gene (OXp/ $\Delta adc1$). PCR analysis employing two pairs of specific primers (Supplementary information Table S1) was used to confirm the accurate integration and placement of each gene fragment into the *Synechocystis* genome. **(A)** The double homologous recombination of both Cm^R gene occurred between the conserved sequences of *psbA2* gene in WTc and $\Delta adc1c$, and a $proC:Cm^R$ fragment occurred between the conserved sequences of *psbA2* gene in OXP and OXP/ $\Delta adc1$ strains when compared to WT. **(B)** For PCR products using UP_*psbA2*-F and Dw_*psbA2*-R primers, **(B.1)** For OXP strain, Lane M: GeneRuler DNA ladder, Lanes OX1, OX2, and OX3: three clones no. 1–3 containing a 3.2 kb fragment of Up_*psbA2*-*proC*- Cm^R -Dw_*psbA2*, Lanes WT and WTc: negative controls of a 2.4 kb fragment in WT and a 2.2 kb fragment in WTc, respectively. **(B.2)** For OXP/ $\Delta adc1$ strain, Lane M: GeneRuler DNA ladder, Lanes OX1 and OX2: two clones no. 1 and 2 containing a 3.2 kb fragment of Up_*psbA2*-*proC*- Cm^R -Dw_*psbA2*, Lanes $\Delta adc1$ and $\Delta adc1c$: negative controls of a 2.4 kb fragment in $\Delta adc1$ and a 2.2 kb fragment in $\Delta adc1c$, respectively. **(C)** For PCR products using ProC-F and Cm^R -R primers, **(C.1)** For OXP strain, Lane M: GeneRuler DNA ladder, Lanes OX1, OX2, and OX3: three clones no. 1–3 containing a 1.9 kb fragment of *proC*- Cm^R , Lanes WT and WTc: negative controls (no band) using WT and WTc as template, respectively. **(C.2)** For OXP/ $\Delta adc1$ strain, Lane M: GeneRuler DNA ladder, Lanes $\Delta adc1$ and $\Delta adc1c$: negative controls (no band) using $\Delta adc1$ and $\Delta adc1c$ as template, respectively, Lanes OX1 and OX2: two clones no. 1 and 2 containing a 1.9 kb fragment of *proC*- Cm^R . **(D)** Transcript levels of *proC* gene determined by RT-PCR using RT-*ProC*-F and RT-*ProC*-R primers (Additional file 1: Table S1) in WT, WTc, $\Delta adc1$, $\Delta adc1c$, and two overexpressing strains, including OXP and OXP/ $\Delta adc1$. The 0.8% agarose gel electrophoresis of PCR products was performed from cells grown for 6 days in normal BG₁₁ medium. The 16s rRNA was used as reference. The cropped gels (in **D**) were taken from the original images of RT-PCR products on agarose gels as shown in Supplementary information Figure S1

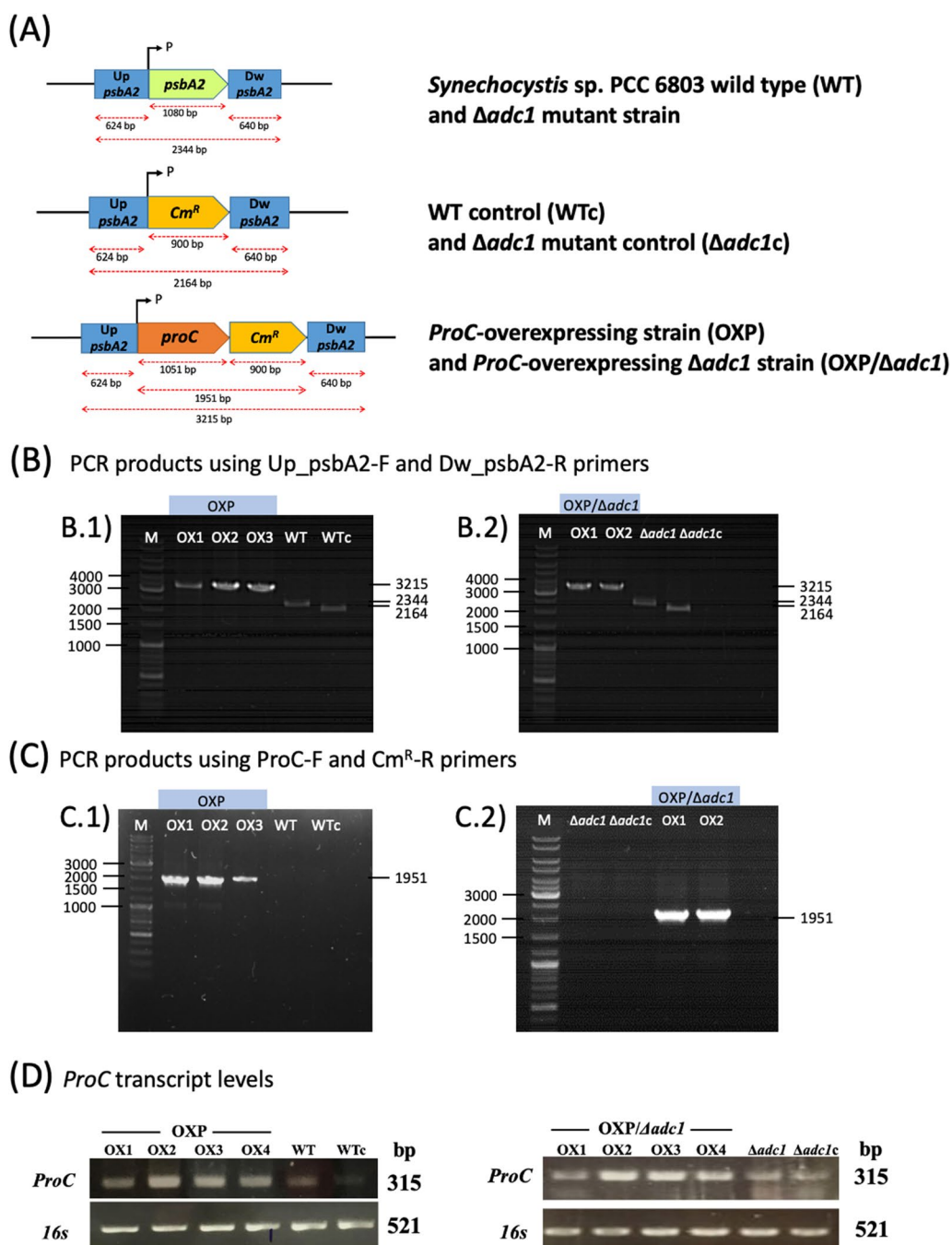


Fig. 2 (See legend on previous page.)

(See figure on next page.)

Fig. 3 Growth curve (A), chlorophyll *a* content (B), carotenoid content (C), oxygen evolution rate (D), contents of polyamines (E), proline (F), glutamate (G), GABA (H), and PHB (I) of WTc, $\Delta adc1c$, OXP, and OXP/ $\Delta adc1$ *Synechocystis sp.* PCC 6803 strains. In (A–C), and (I), cells grown in BG₁₁ medium for 16 days. In (D–H), cells were grown in normal BG₁₁ medium for 7 days, and harvested for metabolite contents. The error bars represent standard deviations of means (mean \pm S.D., $n=3$). In (D–I), the statistical difference of the results between those values of WTc and that engineered strain is indicated by an asterisk at $*P < 0.05$

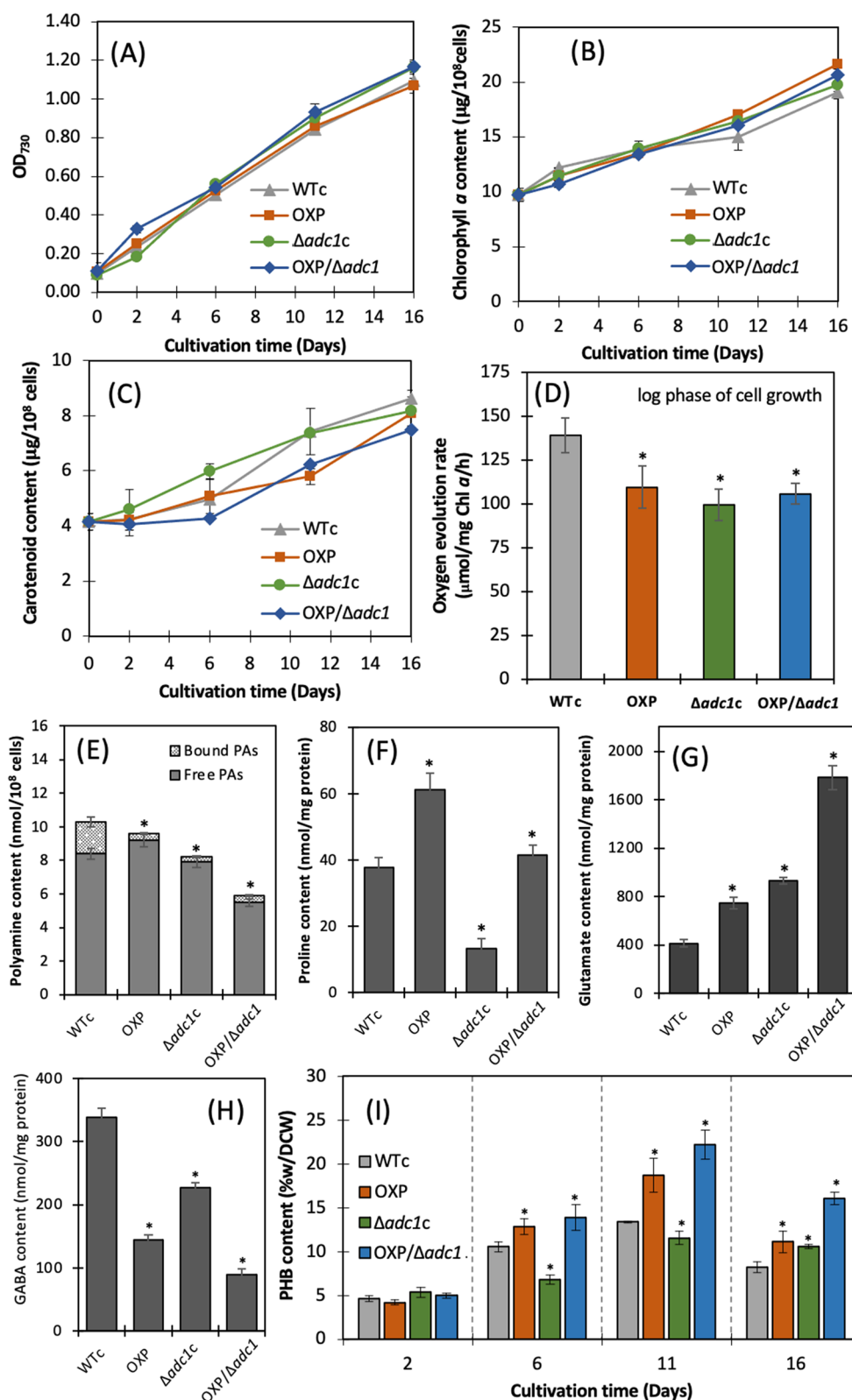


Fig. 3 (See legend on previous page.)

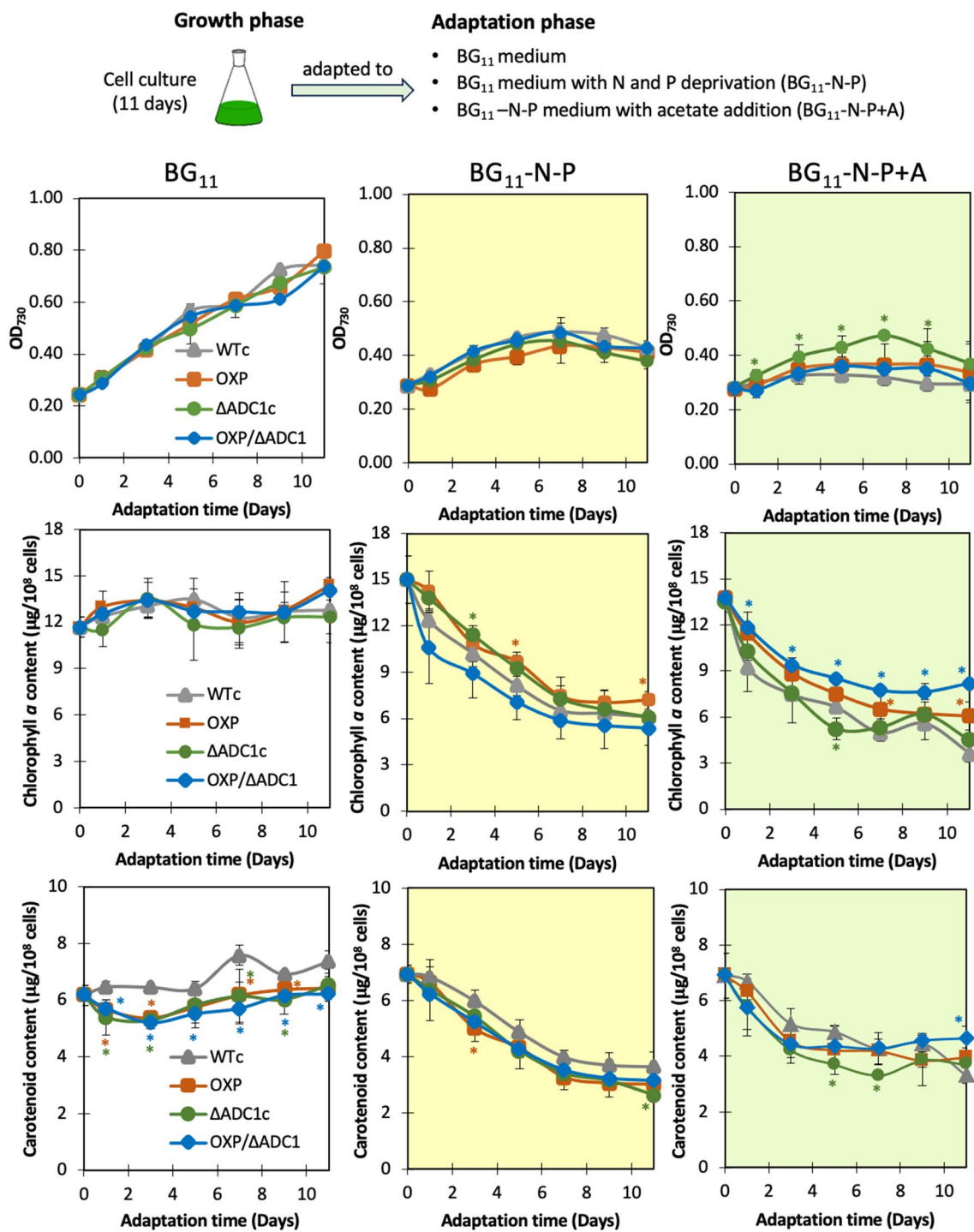


Fig. 4 Growth curve (A–C), chlorophyll *a* content (D–F), and carotenoid content (G–I) of *Synechocystis* WTc, Δ*adc1c*, OXP, and OXP/Δ*adc1* strains adapted in normal BG₁₁ medium, BG₁₁ medium with N and P deprivation (BG₁₁-N-P), and BG₁₁-N-P supplemented with 4%(w/v) acetate (BG₁₁-N-P+A) medium for 11 days. The error bars represent standard deviations of means (mean ± S.D., *n* = 3). The statistical difference of the results between those values of WTc and that engineered strain is indicated by an asterisk at **P* < 0.05

BG₁₁-N-P+A condition, in particular $\Delta adc1c$ (Fig. 4C). In addition, the *proC*-overexpressing strains, including OXP and OXP/ $\Delta adc1$, contained a higher accumulation of chlorophyll a than WTc under the BG₁₁-N-P+A condition (Fig. 4F).

For the main carbon storages of glycogen and polyhydroxybutyrate (PHB) (Fig. 5), glycogen was markedly accumulated rather than PHB under normal growth condition, in particular for a longer period at days 9–11 of cultivation (Fig. 5A and D). The OXP strain contained

the highest level of glycogen, up to 30–49% of dry cell weight, among other strains, during 9–11 days under normal BG₁₁ condition (Fig. 5D). Both BG₁₁-N-P and BG₁₁-N-P+A conditions promoted the specific induction of PHB synthesis in all strains, whereas cells comparatively reduced the quantity of glycogen compared to those under normal condition (Fig. 5B–F). Remarkably, on day 7 of the adaptation phase of both BG₁₁-N-P and BG₁₁-N-P+A media, the OXP/ $\Delta adc1$ strain accumulated the greatest amount of PHB, with around 39.2

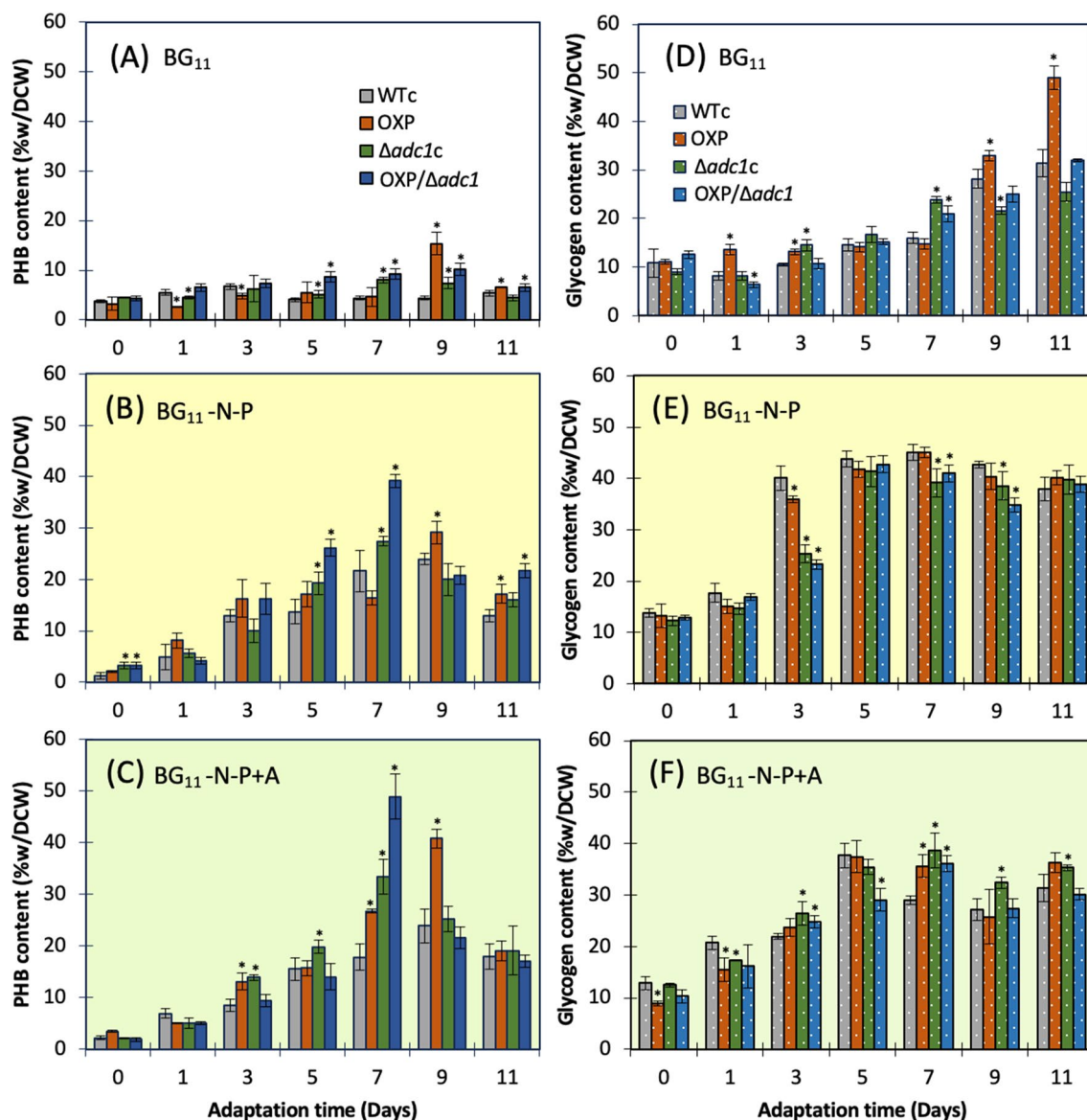


Fig. 5 Contents of PHB (A–C) and glycogen (D–F) of *Synechocystis* WTc, $\Delta adc1c$, OXP, and OXP/ $\Delta adc1$ strains adapted in normal BG₁₁ medium, BG₁₁ medium with N and P deprivation (BG₁₁-N-P), and BG₁₁-N-P supplemented with 4%(w/v) acetate (BG₁₁-N-P+A) medium for 11 days. The error bars represent standard deviations of means (mean \pm S.D., $n = 3$). An asterisk (* $P < 0.05$) denotes the statistical difference in results between those WTc values and that engineered strain at each day

At day 7 of adaptation time

Fold change : [value of OX]/[value of WTc]

Increase
Decrease
Unchanged

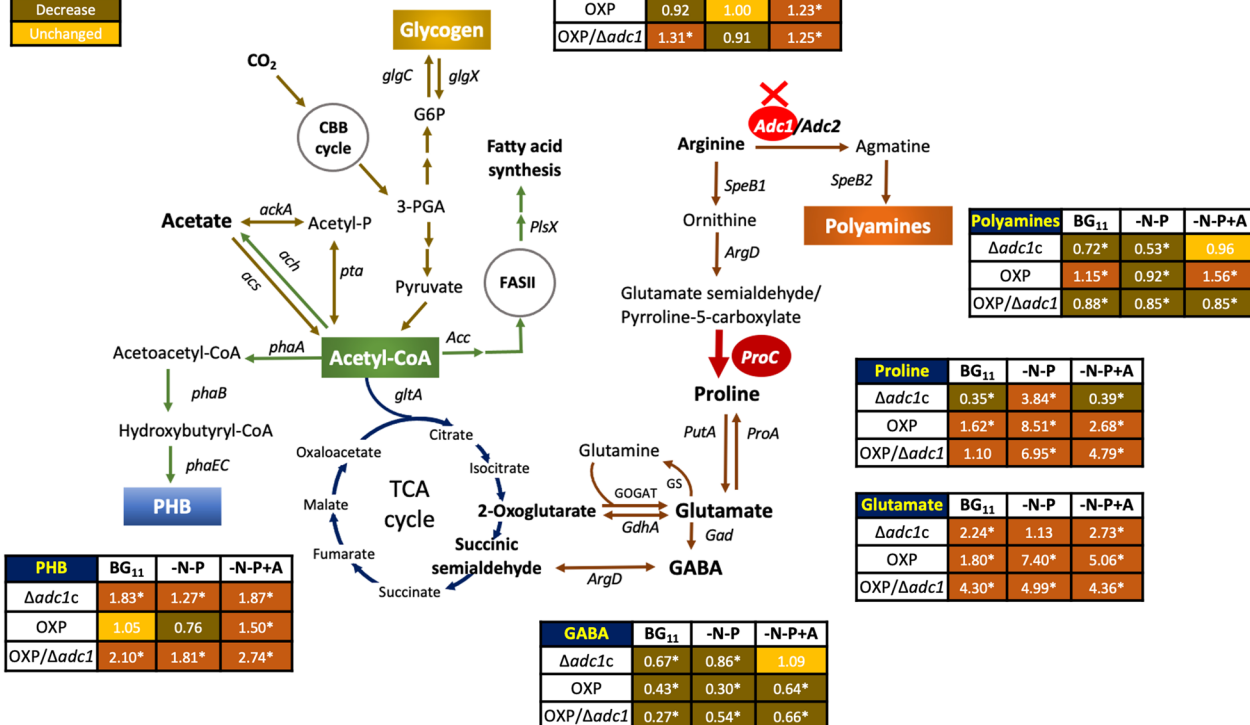


Fig. 6 Fold changes of obtained results of metabolite products in three engineered strains compared with those in *Synechocystis* WTc after adapting cells in BG₁₁, BG₁₁-N-P, and BG₁₁-N-P + A for 7 days. In each box, the number represents the fold change of that value of each engineered strain under each stress condition divided by that value of WTc. The statistical difference in the data between those values of WT and the engineered strain is represented by an asterisk at *P < 0.05

and 48.9%w/DCW, respectively (Fig. 5B, C). Moreover, in Fig. 6, there was a 2.7-fold increase in PHB in the OXP/ $\Delta adc1$ strain compared to WTc at day 7 under a BG₁₁-N-P+A condition. Interestingly, after adapting to both BG₁₁-N-P and BG₁₁-N-P + A media, the PHB accumulation of the OXP strain was later driven to reach its maximum level on day 9. On the other hand, it was anticipated that these BG₁₁-N-P and BG₁₁-N-P + A conditions would result in a reduction in polyamines in all strains, particularly OXP/ $\Delta adc1$ strain (Table 2). It was evident from Fig. 6 that the OXP/ $\Delta adc1$ strain has decreased by 0.8 fold in comparison to WTc (Fig. 6). Regarding the proline-glutamate-GABA pathway, glutamate production predominated under typical BG₁₁ condition, particularly in OXP and OXP/ $\Delta adc1$ strains, followed by GABA and proline (Table 2). The proline content was presumably increased by BG₁₁-N-P and BG₁₁-N-P + A conditions, based on the greater fold change compared to WTc in OXP and OXP/ $\Delta adc1$

strains (Fig. 6). Glutamate accumulation was reduced (Table 2), but in the modified strains, specifically the OXP strain, it increased by more than 5–7 times in both BG₁₁-N-P and BG₁₁-N-P + A conditions, compared to the WTc (Fig. 6). Moreover, GABA accumulation was mostly decreased under nutrient-modified conditions.

We also stained cells adapted under the BG₁₁-N-P + A condition for 7 days with Nile red dye and visualized them under fluorescent microscopy (Fig. 7A). When compared to other strains, the OXP/ $\Delta adc1$ strain manifestly exhibited a high abundance of PHB granules in entire cells. Furthermore, RT-PCR was conducted to measure the transcript levels of 15 different genes (Fig. 7B, C). Both in OXP and OXP/ $\Delta adc1$ under normal and BG₁₁-N-P + A conditions, the *proC* transcript level increased. It is noteworthy that OXP and OXP/ $\Delta adc1$ strains likewise exhibited elevated *putA* transcript levels, encoding proline oxidase. Furthermore, BG₁₁-N-P + A condition increased

Table 2 Contents of some metabolites related to polyamine-proline-glutamate pathway. Cells were grown in various media for 7 days (means \pm S.D., $n=3$). The statistical difference in the data between the values of WT and the engineered strain is represented by an asterisk at $*p < 0.05$

Metabolites/Strains	Contents		
	BG ₁₁ control	BG ₁₁ -N-P	BG ₁₁ -N-P + A
Total polyamine contents (nmol/10 ⁸ cells)			
WTc	12.4 \pm 0.8	7.2 \pm 0.2	5.4 \pm 0.3
Δ <i>adc1c</i>	8.9 \pm 0.6*	3.8 \pm 0.4*	5.2 \pm 0.4
OXp	14.3 \pm 0.5*	6.6 \pm 0.1*	8.4 \pm 0.5*
OXp/ Δ <i>adc1</i>	10.9 \pm 0.2*	6.1 \pm 0.2*	4.6 \pm 0.1*
Proline contents (nmol/mg protein)			
WTc	37.8 \pm 3.0	21.2 \pm 2.0	48.5 \pm 4.0
Δ <i>adc1c</i>	13.2 \pm 0.9*	81.5 \pm 5.0*	19.0 \pm 0.6*
OXp	61.1 \pm 5.4*	180.4 \pm 11.0*	130.0 \pm 10.0*
OXp/ Δ <i>adc1</i>	41.5 \pm 3.0	147.3 \pm 12.0*	232.5 \pm 15.0*
Glutamate contents (nmol/mg protein)			
WTc	415.2 \pm 30.0	38.8 \pm 3.0	58.3 \pm 3.0
Δ <i>adc1c</i>	931.0 \pm 20.0*	43.8 \pm 3.0	159.0 \pm 8.0*
OXp	747.0 \pm 40.0*	287.0 \pm 20.0*	294.8 \pm 15.0*
OXp/ Δ <i>adc1</i>	1784 \pm 70.0*	193.5 \pm 10.0*	253.9 \pm 10.0*
GABA contents (nmol/mg protein)			
WTc	338.0 \pm 10.0	294.8 \pm 9.0	174.6 \pm 5.0
Δ <i>adc1c</i>	226.7 \pm 8.0*	253.0 \pm 8.0*	190.4 \pm 10.0
OXp	144.4 \pm 8.0*	88.5 \pm 6.0*	112.1 \pm 6.0*
OXp/ Δ <i>adc1</i>	89.8 \pm 5.0*	159.5 \pm 10.0*	115.0 \pm 5.0*

the transcript levels of the *gdhA* and *gad* genes, encoding glutamate dehydrogenase and glutamate decarboxylase, respectively, with the exception of the Δ *adc1c* strain. The transcript levels of the *acs*, *ach*, and *ackA* genes, encoding acetyl-CoA synthase, acetyl-CoA hydrolase, and acetate kinase, respectively, in acetate metabolism, were increased by the acetate supplementation in BG₁₁-N-P medium. Remarkably, all strains under the BG₁₁-N-P + A condition showed an increase in the transcript level of the *gltA* gene, encoding citrate synthase in a first step of the TCA cycle, when compared to the normal BG₁₁ condition. On the other hand, although the BG₁₁-N-P + A condition raised the quantity of the *accA* transcript, encoding acetyl-CoA carboxylase subunit A in fatty acid synthesis, relative to the normal condition, there was a low alteration in the *plsX* transcript level, encoding fatty acid/phospholipid synthesis protein. Strikingly, transcript levels of all *pha* genes, including *phaA*, *phaB*, *phaC*, and *phaE*, were upregulated by BG₁₁-N-P + A condition. The reduction of *glgX* transcript amount, encoding glycogen debranching enzyme in glycogen degradation, was induced by the BG₁₁-N-P + A condition rather than the normal BG₁₁ control.

Discussion

The disruption of the polyamine synthetic *adc1* gene in *Synechocystis* sp. PCC 6803 was initially discovered in a previous study [5], but the metabolic regulation remained unclear. In this work, we highlight the remarkable finding that higher PHB synthesis (up to 48.9% of dry cell weight) was caused by enhanced metabolic flux from arginine to proline and glutamate, which is closely related to nutrient stress. The introduction of the native *proC* gene, encoding pyrroline-5-carboxylate reductase of proline synthesis, in *Synechocystis* sp. PCC 6803 wild type (WT) and *adc1* mutant (Δ *adc1*) was constructed, thereby creating OXP and OXP/ Δ *adc1* strains, respectively. The *proC* mutant of *Synechocystis* sp. PCC 6803 was previously shown to produce less proline, but a *putA* mutant that lacks the enzyme proline oxidase, which breaks down proline to glutamate, nonetheless accumulated a high amount of proline metabolites without producing any glutamate [16]. Enhanced proline accumulation is indicated in response to environmental stress [27–29]. In plants, the stress response of proline accumulation was controversial depending on different species and organisms; maize seedlings had an increased proline production in response to nitrogen and phosphorus deficiency [30], while French bean (*Phaseolus vulgaris* L cv Strike) plants showed a decline in proline accumulation under nitrogen-deprived condition [31], as well as a low proline level in *Arabidopsis thaliana* growing under nitrogen-limiting condition [32]. In our study, regarding BG₁₁-N-P and BG₁₁-N-P + A conditions, we found a minor alteration in proline accumulation in WTc as compared to BG₁₁ control (Table 2). It is worthy to note that the *adc1* knockout with a decreased polyamine also contained lower proline content than the WTc, except for the BG₁₁-N-P condition. Our results also indicated that glutamate accumulation in all strains was dramatically decreased in response to nitrogen and phosphorus deprivation in comparison to the WTc. Nevertheless, glutamate content increased more than twofold in all engineered strains as compared to WTc results (Fig. 8), particularly in OXP and OXP/ Δ *adc1* strains. Amidst the deficiency of nitrogen and phosphorus, glutamate might have taken up a rapid key role in the metabolism of amino acids through pathways including the GS/GOGAT pathway, multispecific aminotransferases, GABA synthesis, and reversible conversions to proline and arginine [33–37]. Interestingly, the transcript level of the *gdhA* gene, encoding glutamate dehydrogenase (GDH), was upregulated only in the OXP strain which contained the highest level of glutamate under the BG₁₁-N-P + A condition (Fig. 7B, C), with 1.77-fold increase compared to WTc (Fig. 8). Our finding demonstrated that the *proC* overexpression and *adc1* disruption in *Synechocystis*

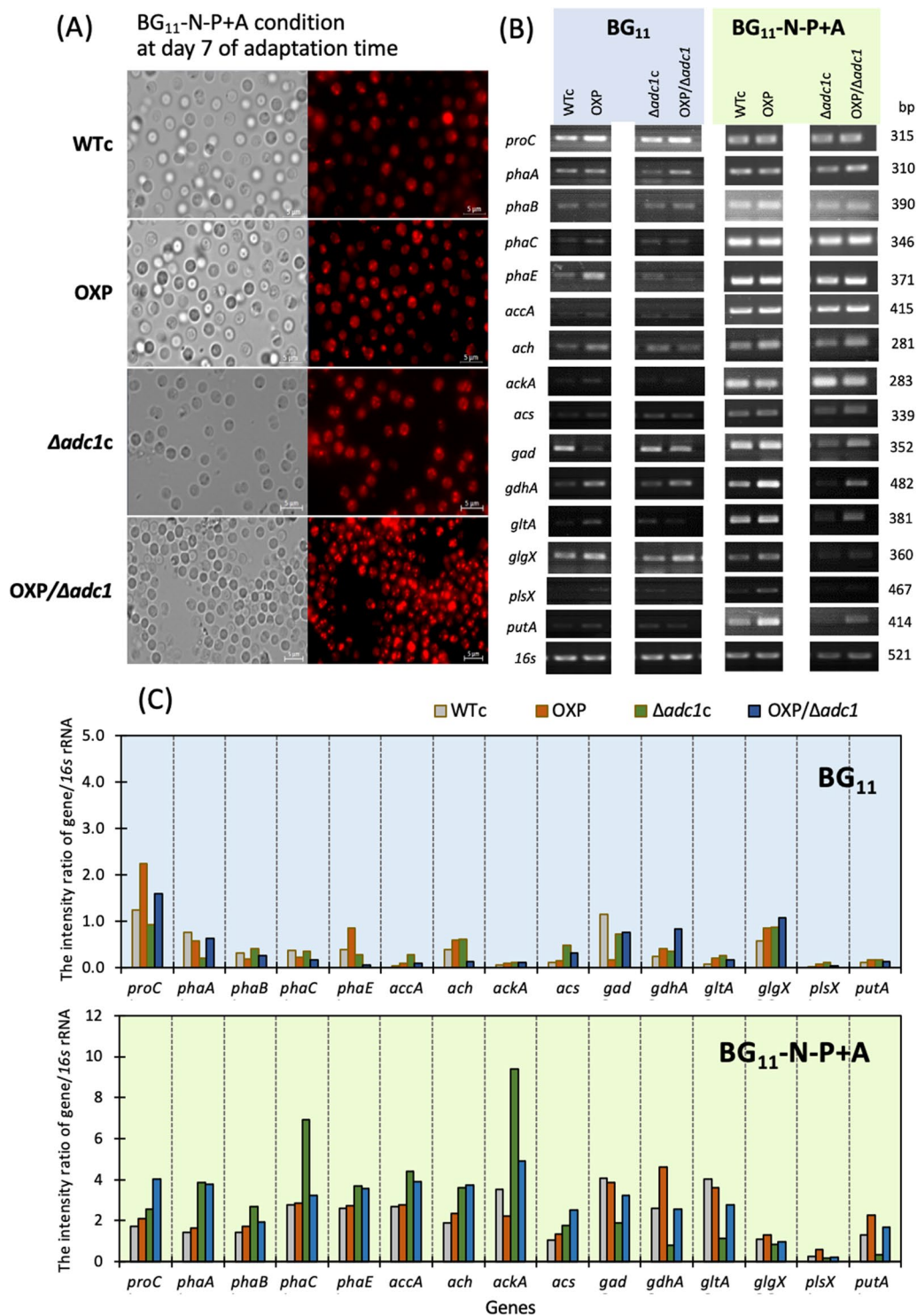


Fig. 7 The Nile red stained PHB granules **(A)**, relative transcript levels **(B)**, and their band intensity ratios of gene/16s **(C)** of genes involved in PHB synthesis, glycogen degradation, proline-glutamate conversion, and neighboring pathways in *Synechocystis* WTc, Δ*adc1c*, OXP, and OXP/Δ*adc1c* strains under BG₁₁-N-P+A condition at day 7 of treatment. The 16s rRNA was used as reference control

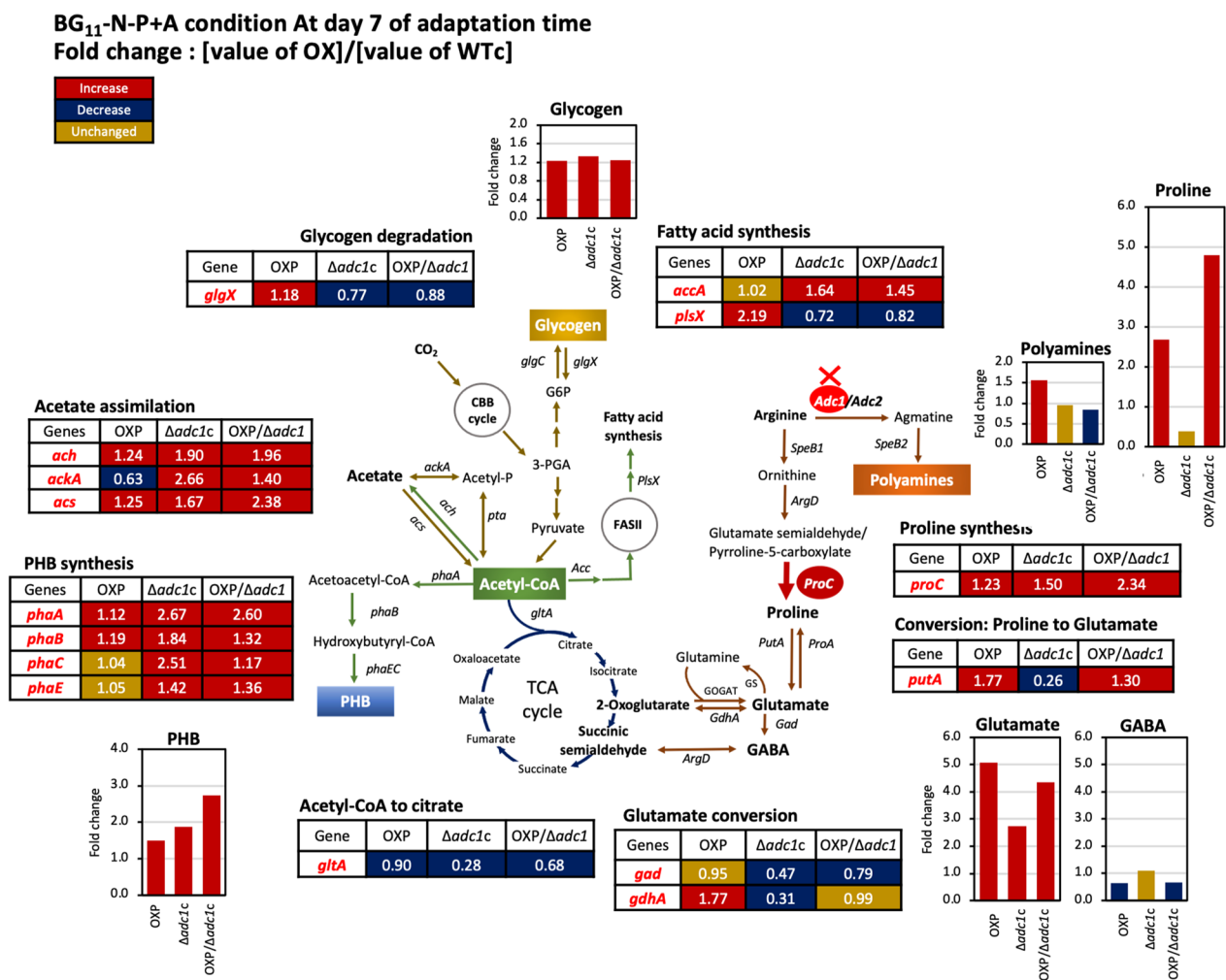


Fig. 8 Fold changes of obtained results of gene transcript levels and metabolite contents in three engineered strains compared with those in *Synechocystis* WTc after adapting cells in BG₁₁-N-P+A for 7 days. In each box and graph, the number and bar graph represents the fold change of that value of each engineered strain divided by that value of WTc, respectively

(OXP/ Δ adc1) had noted results in higher proline and/or glutamate contents in comparison with WTc, which partially alleviated cells under nitrogen and phosphorus deficiency, as evidenced by the increased accumulation of chlorophyll *a*, although the stress effect of nutrient deprivation still existed.

In addition, we demonstrated that, under typical BG₁₁ condition, when cells reached the late phase of growth on day 11, they accumulated more glycogen (Fig. 5D), in particular the OXP strain with 49%w/DCW, and had less PHB (Fig. 5A). The growth phase of cyanobacterial cells, in which the levels of ATP and ADP are elevated during the lag phase and then dropped during the log phase, is directly attributed to the energy charge. The improved metabolism and storage of glycogen significantly contribute to maintaining energy homeostasis [38]. Moreover, the nitrogen and phosphorus deficiency certainly

accelerated the glycogen accumulation within 3 days of the adaptation phase (Fig. 5E), as well as PHB production (Fig. 5B). The impact of glycogen breakdown on PHB synthesis during nitrogen deprivation has been previously reported [8]. Subsequently, in order to improve the acetyl-CoA substrate for PHB synthesis, we added carbon source, herein acetate, to the BG₁₁-N-P medium. On day 7 of the adaptation phase, there was a noticeable increase in PHB accumulation in OXP/ Δ adc1 of around 48.9% w/DCW (Fig. 5C). The increased acetate utilization in the OXP/ Δ adc1 strain in comparison to other strains confirmed this finding (Additional file 1: Fig. S2). Our results indicated that, with the exception of the OXP strain, *Synechocystis* cells favored using exogenous acetate to acetyl-CoA over glycogen breakdown, as demonstrated by a reduced amount of *glgX* transcript under BG₁₁-N-P+A condition (Fig. 7B, C). Regarding acetate

metabolism, cells acclimated to a BG₁₁-N-P medium containing acetate exhibited significantly higher levels of the transcripts *ackA* and *acs*, encoding acetyl-CoA synthase and acetate kinase, respectively. This is consistent with their enhanced fold change, as noted in Fig. 8. It is worth noting that the OXP strain also had a higher *ackA* transcript level than that under normal BG₁₁ medium (Fig. 7B), but it showed a decreased fold change when compared to WTc (Figs. 7C and 8). According to these data, the OXP strain may have utilized acetate less than other strains, which may have contributed to its reduced PHB contents on day 7 under BG₁₁-N-P+A treatment compared to the Δ *adc1c* and OXP/ Δ *adc1* strains. This finding was confirmed by higher amount of acetate remaining in the medium during treatment with the OXP strain than other strains (Additional file 1: Fig. S2). As demonstrated earlier by the *acs* mutant, which did not use the external acetate in medium, it is crucial to stress that the Acs enzyme functions as the primary metabolic route for acetate absorption in *Synechocystis* sp. PCC 6803 [39]. Remarkably, we suggested that the flow of acetyl-CoA metabolite to citrate in the TCA cycle in all strains was induced by the BG₁₁-N-P+A condition, as supported by the upregulated transcript level of *gltA* gene, encoding citrate synthase (Fig. 7B, C). Nonetheless, it is crucial to note that the *gltA* transcript levels in the engineered strains, including OXP, *adc1c*, and OXP/ Δ *adc1*, were lower than the WTc (Fig. 8). This result indicated that the lowered flow of acetyl-CoA to the TCA cycle in engineered strains in comparison to WTc substantially contributed to driving acetyl-CoA to other flux directions, such as PHB biosynthetic pathway and fatty acid synthesis. Then, we postulated that the increased levels of proline and glutamate in the engineered strains OXP, Δ *adc1c*, and OXP/ Δ *adc1* were substantially related to the flow of acetyl-CoA to the TCA cycle and a conversion between 2-oxoglutarate and glutamate. Our results have not provided the TCA cycle's metabolites; further identification of pertinent metabolites or the application of integrative bioinformatic approaches might increase our knowledge of the actual mechanism. For PHB synthesis, it is important to note that all *pha* genes in the PHB synthetic pathway were increased in their transcript amounts under the BG₁₁-N-P+A condition, in particular the *phaC* and *phaE* genes, in comparison to the normal BG₁₁ condition (Fig. 7B, C). Nonetheless, our findings demonstrate a strong correlation between the increased amounts of *phaA* and *phaB* transcripts and the improved synthesis of PHB in the modified strains (OXP, Δ *adc1c*, and OXP/ Δ *adc1*) (Fig. 8). This was in line with a previous study in *Synechocystis* sp. PCC6803, where increased PHB synthesis was associated with overexpression of the

phaAB gene rather than *phaEC* overexpression during nitrogen deprivation [40]. On the other hand, the acetyl-CoA direction to fatty acid synthesis was also induced by the BG₁₁-N-P+A condition due to the high upregulation of the *accA* transcript level and a slight induction of the *plsX* transcript (Fig. 7B, C). This could imply that acetate addition contributes to lipid production in cyanobacteria [40, 41]. According to Ref. [42], cyanobacterial cells grown in high C/low N conditions functioned by preventing the inhibitory interaction of PII protein with ACCase, while cells grown in high N/low C conditions could enhance the PII-ACCase interaction, leading to an inhibition of the ACCase enzyme.

Conclusions

The nitrogen and phosphorus-deprived condition efficiently induced the accumulation of glycogen and PHB in *Synechocystis* sp. PCC 6803. In this study, higher PHB production was attained in three modified *Synechocystis* sp. PCC6803 strains, including Δ *adc1c*, OXP, and OXP/ Δ *adc1*, under the nutrient-deprived treatments, in particular nitrogen and phosphorus-deprived BG₁₁ medium with acetate addition (BG₁₁-N-P+A). The *proC* overexpression and *adc1* knockout in *Synechocystis* apparently induced the changes in proline and glutamate contents inside the cells, which partially alleviated cells under nitrogen and phosphorus deprivation. However, the acetate addition, enhancing acetyl-CoA metabolite, significantly boosted the PHB and glycogen storage. These genetically modified strains of *Synechocystis* (Δ *adc1c*, OXP, and OXP/ Δ *adc1*) might serve as practicable cell factories for biotechnological applications including biomaterials and biofuels.

Materials and Methods

Construction of *proC*-overexpressing *Synechocystis* sp. PCC 6803

First, the recombinant plasmid pEERM_*ProC* was constructed (Table 1), which was naturally transformed into *Synechocystis* sp. PCC 6803 wild type (WT) and Δ *adc1* mutant (obtained from [5]), thereby generating a *proC*-overexpressing *Synechocystis* sp. PCC 6803 (OXP), and an OXP lacking *adc1* gene (OXP/ Δ *adc1*), respectively. The pEERM_*proC* plasmid was constructed by ligating the *proC* gene fragment amplified by PCR using a pair of ProC-F and ProC-R primers, as shown in Additional file 1: Table S1, in between the *SpeI* and *PstI* restriction sites in the pEERM vector [26]. The correct recombinant plasmid pEERM_*proC* was transformed into WT and Δ *adc1* mutant cells by natural transformation to create OXP and OXP/ Δ *adc1* strains, respectively. In addition, we also constructed the *Synechocystis* sp. PCC 6803

wild-type control (WTc) and the $\Delta adc1$ mutant control ($\Delta adc1c$) by transforming the empty pEERM vector into WT and $\Delta adc1$ cells, represented as *Synechocystis* WT or $\Delta adc1$ mutant containing the Cm^R cassette gene (Fig. 2A). For host cell suspension preparation, the host cells (WT or $\Delta adc1$) were cultured in BG₁₁ medium until OD₇₃₀ reaching about 0.3–0.5. Then, 10 mL of cell culture was harvested by centrifugation at 5500 rpm (3505×g), 25 °C for 10 min, and cell pellets were resuspended in 500 µL of new BG₁₁ medium. Next step, the host cell suspension was mixed with 10 µL of recombinant plasmid solution, and incubated that mixture overnight in the culture room with continuous light illumination at 40–50 µE/m²/s, at 28–30 °C. Then, the sample mixture was spread on a BG₁₁ agar plate containing 10 µg/mL of chloramphenicol, and incubated in the culture room for 2–3 weeks until survived colonies occurred on plate. Each single colony was picked and streaked on a new BG₁₁ agar plate containing higher concentrations of chloramphenicol (20 and 30 µg/mL), and incubated under same condition until transformant colonies appeared. The obtained transformants were confirmed for gene size, location, and segregation by PCR method using many specific pairs of primers (Additional file 1: Table S1).

Strains and culture conditions

Synechocystis sp. PCC 6803 wild type (WT), derived from the Berkeley strain 6803 from fresh water in California, USA [43], *Synechocystis* lacking *adc1* gene ($\Delta adc1$), and all engineered strains (WTc, $\Delta adc1c$, OXP, and OXP/ $\Delta adc1$) were grown in normal BG₁₁ medium for 16 days. The culture room, set for normal growth condition, was performed at 28–30 °C, with a continuous white light illumination by 40–50 µE/m²/s intensity. The cell culture flasks with the initial cell density at 730 nm (OD₇₃₀) of about 0.05 were placed on the rotary shaker at 160 rpm speed. Cell growth was measured at OD₇₃₀ by spectrophotometer. For nutrient-deprived conditions, all *Synechocystis* strains were initially grown in normal BG₁₁ medium until late-log phase of cell growth before treating them with nutrient-derived media under the same growth condition for 11 days. There were two modified media including a BG₁₁ medium without nitrogen (N) and phosphorus (P) (or BG₁₁-N-P), and a BG₁₁-N-P medium with 0.4%(w/v) acetate (A) addition (or BG₁₁-N-P+A). For BG₁₁-N-P medium, it was a BG₁₁ medium lacking NaNO₃ with KCl added in place of KH₂PO₄, and FeSO₄ added in place of ferric ammonium citrate in equimolar concentrations [5]. In addition, the initial OD₇₃₀ of cell culture under nutrient-modified conditions was adjusted to about 0.2. Acetate concentration in medium was determined according to the method of Ref. [44].

Determinations of intracellular pigments and oxygen evolution rate

Cell culture (1 mL) was harvested by centrifugation at 12,000 rpm (14,383×g) for 10 min. The intracellular pigments including chlorophyll *a* and carotenoids in cell pellets were extracted by N,N-dimethylformamide (DMF) (1 mL), vortexed and incubated under darkness for 10 min. After centrifugation at the same speed, the absorbance of the yellowish supernatant was spectrophotometrically measured at 461, 625, and 664 nm. The contents of chlorophyll *a* and carotenoids were calculated according to Refs. [45, 46]. For oxygen evolution rate, cell culture (10 mL) was harvested by centrifugation at 5500 rpm (3505×g), 25 °C for 10 min. Cell pellets were resuspended in new BG₁₁ medium (1 mL) and incubated under darkness for 30 min before measuring the oxygen evolution. Saturated light source was employed at 25 °C using Clark-type oxygen electrode (Hansatech instruments Ltd., King's Lynn, UK). The unit of oxygen evolution rate was addressed as µmol O₂/mg chlorophyll a/h [5].

Total RNAs extraction and reverse transcription-polymerase reaction (RT-PCR)

Total RNAs were extracted from *Synechocystis* cells using the TRIzol[®] Reagent (Invitrogen, Life Technologies Corporation, Carlsbad, CA, USA). The purified RNAs (1 µg) were converted to cDNA by reverse transcription using ReverTra ACE[®] qPCR RT Master Mix Kit (TOYOBO Co., Ltd., Osaka, Japan). This obtained cDNA was subsequently used as a template for PCR with different pairs of primers (Additional file 1: Table S1). The PCR conditions were performed by initial denaturing at 95 °C for 5 min, followed by 30 cycles of 95 °C for 30 s, annealing temperature of each gene (Additional file 1: Table S1) for 30 s, and 72 °C for 35 s, followed by a final extension at 72 °C for 5 min. For 16s rRNA reference, the PCR condition was the same, but there was 19 cycles instead. Prior to initiating the experiment, the optimum cycle for all genes was determined. Those bands were not saturated; instead, they were in the appropriate cycle. The PCR products were checked by 1.5% (w/v) agarose gel electrophoresis. Quantification of band intensity was detected by Syngene[®] Gel Documentation (Syngene, Frederick, MD, USA).

HPLC analysis of PHB contents and Nile red staining

Cell cultures (50 mL) were harvested by centrifugation at 5500 rpm (3505×g) for 10 min. To prepare sample for HPLC detection, cell pellets were hydrolyzed by boiling for 60 min with 98%(v/v) sulfuric acid (800 µL) and 20 mg/mL adipic acid (100 µL), an internal standard [5]. After that, the hydrolyzed sample was filtered using a

0.45 μm polypropylene membrane filter which was further detected by HPLC instrument (Shimadzu HPLC LGE System, Kyoto, Japan) using a carbon-18 column, Inert sustain 3- μm (GL Science, Tokyo, Japan), with a UV detector at 210 nm. The running buffer consisted of 30% (v/v) acetonitrile dissolved in 10 mM KH_2PO_4 (pH 7.4), with a flow rate of 1.0 mL/min. Authentic commercial PHB was used as standard, which was prepared as same as the samples. For dry cell weight (DCW), it was determined by incubating cell pellets in an oven at 80 °C for 16–18 h, until obtaining the constant weight.

For Nile red staining, cell culture (1 mL) was harvested by centrifugation at 5500 rpm (3505 \times g) for 10 min. Cell pellets were resuspended in Nile red staining solution (3 μL). Then, the addition of normal saline (0.9%, w/v, 100 μL) was conducted and incubated overnight under darkness [5, 40]. To visualize the stained cells, fluorescent microscope (Carl Zeiss, Oberkochen, Jena, Germany) was applied using a filter cup with 535 excitation wavelength, at a magnification of 100x.

Extraction and determination of glycogen content

Harvested cell pellets from liquid culture (15–30 mL) were extracted by alkaline hydrolysis [47, 48]. The 30% potassium hydroxide (KOH) solution (400 μL) was mixed with cell pellets, and boiled for 1 h. After centrifugation at 12,000 rpm (14,383 \times g), 4 °C for 10 min, the supernatant was transferred to a new tube and mixed with 900 μL of cold absolute ethanol before incubating at – 20 °C overnight to precipitate glycogen. Next step, the sample mixture was centrifuged at 12,000 rpm (14,383 \times g), 4 °C for 30 min to obtain glycogen pellets which were subsequently dried at 60 °C overnight. Glycogen pellets were dissolved in 1 mL of 10% H_2SO_4 . Then, dissolved sample (0.2 mL) was mixed with 10% H_2SO_4 (0.2 mL) and anthrone reagent (0.8 mL) before boiling for 10 min. After cooling down the samples to room temperature, the absorbance of samples was measured at 625 nm by spectrophotometer (modified from [4, 7]). A commercial oyster glycogen was used as the standard which was prepared as similar as the sample. The unit of glycogen content was %w/DCW.

Extraction and determination of polyamine content

Total polyamines were extracted from *Synechocystis* cells with 5% cold HClO_4 (modified from [49, 50]). After extraction by 5% cold HClO_4 for 1 h on ice, the extracted samples were centrifuged at 12,000 rpm (14,838 \times g) for 10 min. The supernatant and pellet fractions were represented as the fraction containing free and bound forms of polyamines, respectively. Both fractions were used to derivatize and quantify the total polyamines. For the derivatization, it was performed with benzoyl chloride

using 1,6-hexanediamine as an internal standard. 1 mL of 2 M NaOH was mixed with 500 μL of HClO_4 extract and 10 μL of benzoyl chloride. After vigorously mixing, the mixture was incubated for 20 min at room temperature. To terminate the reaction, saturated NaCl solution (2 mL) was added. The benzoyl polyamines were subsequently extracted by cold diethyl ether (2 mL). In addition, the ether phase (1 mL) was evaporated to dryness, and redissolved in methanol (1 mL). Authentic polyamine standards were prepared as similar as the samples. The polyamine content was detected by high-performance liquid chromatography (HPLC; Shimadzu HPLC LGE System, Kyoto, Japan) with inertsil[®] ODS-3 C-18 reverse phase column (5 μm ; 4.6 \times 150 mm) with UV–Vis detector at 254 nm. The mobile phase was a gradient of 60–100% methanol with a flow rate of 0.5 mL/min.

Quantification of proline, glutamate, and GABA contents

HPLC detection of amino acids, including proline, glutamate, and GABA, was performed using *o*-phthalaldehyde (OPA) and 9-Fluorenylmethyl chloroformate (FMOC) derivatives (modified from [51, 52]). Cell pellets obtained from cell culture (50 mL) were washed and resuspended in 10 mM potassium phosphate citrate buffer (pH 7.6). Cell suspensions were homogenized using SONOPLUS Ultrasonic homogenizer (BANDELIN electronic GmbH & Co., Berlin, Germany). The supernatant was collected after centrifugation at 12,000 rpm (14,838 \times g) for 10 min, and concentrated by a Centrivap concentrator (Labconco Corporation, MO, USA). The concentrated sample was further extracted with 600 μL of a mixture of water:chloroform:methanol (3:5:12, v/v/v), followed by 300 μL of chloroform and 450 μL of distilled water before centrifugation again at 5500 rpm (3505 \times g), 4 °C, for 10 min. The upper fraction of water–methanol phase was collected, and evaporated before redissolving in 200 μL of 0.1 N HCl. The sample solution was filtered through a 0.45 μm membrane filter, and then diluted (1:4, v/v) with internal standard solution of norvaline and sarcosine (62.5 mM in 0.1 M HCl). Then, this mixture was again filtered through a 0.45 μm membrane filter before detecting by HPLC with UV–VIS detector (Shimadzu HPLC LGE System, Kyoto, Japan) using 4.6 \times 150 mm, 3.5 μm Agilent Zorbax Eclipse AAA analytical column and 4.6 \times 12.5 mm, 5.0 μm guard column (Agilent Technologies, CA, USA). For the mobile phase, eluent A was 40 mM Na_2HPO_4 , pH 7.8, and eluent B was acetonitrile:methanol:water (45:45:10, v/v/v), with a flow rate of 2 mL/min. The OPA- and FMOC-derivatized amino acids were monitored at 338 and 262 nm, respectively. The unit of amino acid content was nmol/mg protein.

Abbreviations

ADC	Arginine decarboxylase
Arg	Arginine
Car	Carotenoids
Chl <i>a</i>	Chlorophyll <i>a</i>
DCW	Dry cell weight
DMF	N,N-Dimethylformamide
Fmoc	9-Fluorenylmethyl chloroformate
GABA	Gamma-aminobutyric acid
h	Hour
µg	Microgram
mL	Milliliter
min	Minute
nm	Nanometer
OD	Optical density
OPA	O-Phthalaldehyde
PCR	Polymerase chain reaction
PHB	Polyhydroxybutyrate
rpm	Revolutions per minute
s	Seconds
WT	Wild type

Supplementary Information

The online version contains supplementary material available at <https://doi.org/10.1186/s13068-024-02458-9>.

Additional file 1: Table S1. Primers used in this study. **Figure S1.** Agarose gel electrophoresis of RT-PCR products of proC transcript in *Synechocystis* sp. PCC 6803 strains grown under normal BG11 condition for 6 days, shown in Figure 2C. The 16S rRNA transcript was used as the reference (a size of 521 bp). ProC transcript size of 315 bp. **Figure S2.** Acetate concentration in BG11-N-P+A medium during adaptation phase of all strains. Cells were treated in BG11-N-P+A medium for 11 days. Medium was sampled at days 0, 1, 3, 5, 7, 9, and 11 for determining acetate concentration (according to the method of Hutchens and Kass, 1949). The error bars represent standard deviations of means (mean ± S.D., n = 3).

Acknowledgements

We gratefully thank Professor Peter Lindblad, Microbial Chemistry, Department of Chemistry–Ångström, Uppsala University, for providing the expression vector pEERM for our work.

Author contributions

SU responsible for study conception, experimenter, data collection and analysis, manuscript preparation. SJ study conception, supervision, and design, critical revision and manuscript writing, and final approval of the manuscript. All the authors read and approved the final manuscript.

Funding

This research was supported by the 90th Anniversary of Chulalongkorn University Fund (Ratchadaphiseksomphot Endowment Fund) to S.U. and S.J. This Research is also funded by Thailand Science research and Innovation Fund Chulalongkorn University (CU_FRB65_heal(66)_129_23_59) to S.J.

Availability of data and materials

Data generated and analyzed during this study are included in the published article.

Declarations**Ethics approval and consent to participate**

Not applicable.

Consent for publication

Not applicable. All the authors agree to the submission and publication of this manuscript.

Competing interests

The authors declare that they have no competing interests.

Received: 31 October 2023 Accepted: 5 January 2024

Published online: 13 January 2024

References

- Sutherland DL, McCauley J, Labeeuw L, Ray P, Kuzhiumparambil U, Hall C, Doblin M, Nguyen LN, Ralph PJ. How microalgal biotechnology can assist with the UN Sustainable Development Goals for natural resource management. *Curr Res Environ Sustain.* 2021;3: 100050. <https://doi.org/10.1016/j.crsust.2021.100050>.
- Pathak J, Maurya PK, Singh SP, Häder D-P, Sinha RP. Cyanobacterial farming for environment friendly sustainable agriculture practices: innovations and perspectives. *Front Environ Sci.* 2018;6:7. <https://doi.org/10.3389/fenvs.2018.00007>.
- Natesungnoen M, Pongrakhananon V, Lindblad P, Jantaro S. Overexpressing carotenoid biosynthetic genes in *Synechocystis* sp. PCC 6803 improved intracellular pigments and antioxidant activity, which can decrease the viability and proliferation of lung cancer cells in vitro. *Int J Mol Sci.* 2023;24:9370. <https://doi.org/10.3390/ijms24119370>.
- Tharasirivat V, Jantaro S. Increased biomass and polyhydroxybutyrate production by *Synechocystis* sp. PCC 6803 overexpressing RuBisCO genes. *Int J Mol Sci.* 2023;24:6415. <https://doi.org/10.3390/ijms24076415>.
- Utharn S, Yodsang P, Incharoensakdi A, Jantaro S. Cyanobacterium *Synechocystis* sp. PCC 6803 lacking *adc1* gene produces higher polyhydroxybutyrate accumulation under modified nutrients of acetate supplementation and nitrogen-phosphorus starvation. *Biotechnol Rep.* 2021;31:e00661. <https://doi.org/10.1016/j.btre.2021.e00661>.
- Eungrasamee K, Incharoensakdi A, Lindblad P, Jantaro S. Overexpression of *lipA* or *glpD*_RuBisCO in the *Synechocystis* sp. PCC 6803 mutant lacking the *Aas* gene enhances free fatty-acid secretion and intracellular lipid accumulation. *Int J Mol Sci.* 2021;22:11468. <https://doi.org/10.3390/ijms22111468>.
- Eungrasamee K, Lindblad P, Jantaro S. Enhanced productivity of extracellular free fatty acids by gene disruptions of acyl-ACP synthetase and S-layer protein in *Synechocystis* sp. PCC 6803. *Biotechnol Biofuels Bioprod.* 2022;15:99. <https://doi.org/10.1186/s13068-022-02197-9>.
- Koch M, Doello S, Gutekunst K, Forchhammer K. PHB is produced from glycogen turn-over during nitrogen starvation in *Synechocystis* sp. PCC 6803. *Int J Mol Sci.* 2019;20:1942. <https://doi.org/10.3390/ijms20081942>.
- Osanai T, Oikawa A, Numata K, Kuwahara A, Iijima H, Doi Y, Saito S, Hirai MY. Pathway-level acceleration of glycogen catabolism by a response regulator in the cyanobacterium *Synechocystis* species PCC 6803. *Plant Physiol.* 2014;164(4):1831–41. <https://doi.org/10.1104/pp.113.232025>.
- Iwaki T, Haranoh K, Inoue N, Kojima K, Satoh R, Nishino T, Wada S, Ihara H, Tsuyama S, Kobayashi H, Wadano A. Expression of foreign type I ribulose-1,5-bisphosphate carboxylase/oxygenase (EC 4.1.1.39) stimulates photosynthesis in cyanobacterium *Synechococcus* PCC7942 cells. *Photosynth Res.* 2006;88:287–97. <https://doi.org/10.1007/s11120-006-9048-x>.
- Liang F, Lindblad P. *Synechocystis* PCC 6803 overexpressing *RuBisCO* grow faster with increased photosynthesis. *Metab Eng Commun.* 2017;4:29–36. <https://doi.org/10.1016/j.meteno.2017.02.002>.
- Kanno M, Carroll AL, Atsumi S. Global metabolic rewiring for improved CO₂ fixation and chemical production in cyanobacteria. *Nat Commun.* 2017;8:14724. <https://doi.org/10.1038/ncomms14724>.
- Joseph A, Aikawa S, Sasaki K, Teramura H, Hasunuma T, Matsuda F, Osanai T, Hirai MY, Kondo A. Rre37 stimulates accumulation of 2-oxoglutarate and glycogen under nitrogen starvation in *Synechocystis* sp. PCC 6803. *FEBS Lett.* 2014;588(3):466–71. <https://doi.org/10.1016/j.febslet.2013.12.008>.
- Hauf W, Schlebusch M, Hüge J, Kopka J, Hagemann M, Forchhammer K. Metabolic changes in *Synechocystis* PCC6803 upon nitrogen-starvation: excess NADPH sustains polyhydroxybutyrate accumulation. *Metabolites.* 2013;3:101–18. <https://doi.org/10.3390/metabo3010101>.
- Hickman J, Kotovic KM, Miller C, Warrenner P, Kaiser B, Jurista T, Budde M, Cross F, Roberts JM, Carleton M. Glycogen synthesis is a required component of the nitrogen stress response in *Synechococcus elongatus*

- PCC 7942. *Algal Res.* 2013;2:98–106. <https://doi.org/10.1016/j.algal.2013.01.008>.
16. Quintero MJ, Muro-Pastor AM, Herrero A, Flores E. Arginine catabolism in the cyanobacterium *Synechocystis* sp. strain PCC 6803 involves the urea cycle and arginase pathway. *J Bacteriol.* 2000;182(4):1008–15. <https://doi.org/10.1128/jb.182.4.1008-1015.2000>.
 17. Flores E. Studies on the regulation of arginine metabolism in cyanobacteria should include mixotrophic conditions. *MBio.* 2021;12(3):e01433–e1521. <https://doi.org/10.1128/mbio.01433-21>.
 18. Tyo KE, Jin YS, Espinoza FA, Stephanopoulos G. Identification of gene disruptions for increased poly-3-hydroxybutyrate accumulation in *Synechocystis* PCC 6803. *Biotechnol Prog.* 2009;25:1236–43. <https://doi.org/10.1002/btpr.228>.
 19. Neilson AH, Doudoroff M. Ammonia assimilation in blue-green algae. *Archiv Mikrobiol.* 1973;89:15–22. <https://doi.org/10.1007/BF00409395>.
 20. Muro-Pastor MI, Florencio F. Regulation of ammonium assimilation in cyanobacteria. *Plant Physiol Biochem.* 2003;41(6–7):595–603. [https://doi.org/10.1016/S0981-9428\(03\)00066-4](https://doi.org/10.1016/S0981-9428(03)00066-4).
 21. Chávez S, Reyes JC, Chauvat F, Florencio FJ, Candau P. The NADP-glutamate dehydrogenase of the cyanobacterium *Synechocystis* 6803: cloning, transcriptional analysis and disruption of the *gdhA* gene. *Plant Mol Biol.* 1995;28:173–88. <https://doi.org/10.1007/BF00042048>.
 22. Chávez S, Lucena JM, Reyes JC, Florencio FJ, Cancau P. The presence of glutamate dehydrogenase is a selective advantage for the cyanobacterium *Synechocystis* sp. strain PCC 6803 under nonexponential growth conditions. *J Bacteriol.* 1999;181(3):808–13. <https://doi.org/10.1128/jb.181.3.808-813.1999>.
 23. Helling RB. Why does *Escherichia coli* have two primary pathways for synthesis of glutamate? *J Bacteriol.* 1994;176:4664–8. <https://doi.org/10.1128/jb.176.15.4664-4668.1994>.
 24. Hein S, Tran H, Steinbüchel A. *Synechocystis* sp. PCC6803 possesses a two component polyhydroxyalkanoic acid synthase similar to that of anoxygenic purple sulfur bacteria. *Arch Microbiol.* 1998;170:162–70. <https://doi.org/10.1007/s002030050629>.
 25. Dutt V, Srivastava S. Novel quantitative insights into carbon sources for synthesis of poly hydroxybutyrate in *Synechocystis* PCC 6803. *Photosynth Res.* 2018;136:303–14. <https://doi.org/10.1007/s11120-017-0464-x>.
 26. Englund E, Andersen-Ranberg J, Miao R, Hamberger B, Lindberg P. Metabolic engineering of *Synechocystis* sp. PCC 6803 for production of the plant diterpenoid manoyl oxide. *ACS Synth Biol.* 2015;4(12):1270–8. <https://doi.org/10.1021/acssynbio.5b00070>.
 27. Szabados L, Savouré A. Proline: a multifunctional amino acid. *Trends Plant Sci.* 2010;15(2):89–97. <https://doi.org/10.1016/j.tplants.2009.11.009>.
 28. Singh P, Tiwari A, Singh SP, Asthana RK. Proline biosynthesizing enzymes (glutamate 5-kinase and pyrroline-5-carboxylate reductase) from a model cyanobacterium for desiccation tolerance. *Physiol Mol Biol Plants.* 2013;19(4):521–8. <https://doi.org/10.1007/s12298-013-0186-2>.
 29. Spormann S, Nadais P, Sousa F, Pinto M, Martins M, Sousa B, Fidalgo F, Soares C. Accumulation of proline in plants under contaminated soils—are we on the same page? *Antioxidants.* 2023;12(3):666. <https://doi.org/10.3390/antiox12030666>.
 30. Göring H, Thien BH. Influence of nutrient deficiency on proline accumulation in the cytoplasm of *Zea mays* L seedlings. *Biochem Physiol Pflanzen.* 1979;174(1):9–16. [https://doi.org/10.1016/S0015-3796\(17\)30541-3](https://doi.org/10.1016/S0015-3796(17)30541-3).
 31. Sánchez E, Ruiz JM, Romeo L. The response of proline metabolism to nitrogen deficiency in pods and seeds of French bean (*Phaseolus vulgaris* L cv Strike) plants. *J Sci Food Agric.* 2001;81(15):1471–5. <https://doi.org/10.1002/jsfa.966>.
 32. Lemaître T, Gauffichon L, Boutet-Mercey S, Christ A, Masclaux-Daubresse C. Enzymatic and metabolic diagnostic of nitrogen deficiency in *Arabidopsis thaliana* Wassilewskija accession. *Plant Cell Physiol.* 2008;49(7):1056–65. <https://doi.org/10.1093/pcp/pcn081>.
 33. Muro-Pastor MI, Reyes JC, Florencio F. Cyanobacteria perceive nitrogen status by sensing intracellular 2-oxoglutarate levels. *J Biol Chem.* 2001;276(41):38320–8. <https://doi.org/10.1074/jbc.M105297200>.
 34. Herrero A, Muro-Pastor AM, Flores E. Nitrogen control in cyanobacteria. *J Bacteriol.* 2001;183(2):411–25. <https://doi.org/10.1128/jb.183.2.411-425.2001>.
 35. Forde BG, Lea PJ. Glutamate in plants: metabolism, regulation, and signaling. *J Exp Bot.* 2007;58(9):2339–58. <https://doi.org/10.1093/jxb/erm121>.
 36. Forchhammer K, Schwarz R. Nitrogen chlorosis in unicellular cyanobacteria—a developmental program for surviving nitrogen deprivation. *Environ Microbiol.* 2019;21(4):1173–84. <https://doi.org/10.1111/1462-2920.14447>.
 37. Yang TY, Li H, Tai Y, Dong C, Cheng X, Xia E, Chen Z, Li F, Wan X, Zhang Z. Transcriptional regulation of amino acid metabolism in response to nitrogen deficiency and nitrogen forms in tea plant root (*Camellia sinensis* L.). *Sci Rep.* 2020;10:6868. <https://doi.org/10.1038/s41598-020-63835-6>.
 38. Cano M, Holland SC, Artier J, Burnap RL, Ghirardi M, Morgan JA, Yu J. Glycogen synthesis and metabolite overflow contribute to energy balancing in cyanobacteria. *Cell Rep.* 2018;23:667–72. <https://doi.org/10.1016/j.celrep.2018.03.083>.
 39. Du W, Jongbloets JA, van Boxtel C, Hernández HP, Lips D, Oliver BG, Hellingwerf KJ, dos Santos FB. Alignment of microbial fitness with engineered product formation: obligatory coupling between acetate production and photoautotrophic growth. *Biotechnol Biofuels.* 2018;11:38. <https://doi.org/10.1186/s13068-018-1037-8>.
 40. Khetkorn W, Incharoensakdi A, Lindblad P, Jantaro S. Enhancement of poly-3-hydroxybutyrate production in *Synechocystis* sp. PCC 6803 by overexpression of its native biosynthetic genes. *Bioresour Technol.* 2016;214:761–8. <https://doi.org/10.1016/j.biortech.2016.05.014>.
 41. Towijit U, Songruk N, Lindblad P, Incharoensakdi A, Jantaro S. Co-overexpression of native phospholipid-biosynthetic genes *plsX* and *plsC* enhances lipid production in *Synechocystis* sp. PCC 6803. *Sci Rep.* 2018;8:13510. <https://doi.org/10.1038/s41598-018-31789-5>.
 42. Forchhammer K, Selim KA. Carbon/nitrogen homeostasis control in cyanobacteria. *FEMS Microbiol Rev.* 2020;44(1):33–53. <https://doi.org/10.1093/femsre/fuz025>.
 43. Stanier RY, Kunisawa R, Mandel M, Cohen-Bazire G. Purification and properties of unicellular blue-green alga (order Chroococcales). *Bacteriol Rev.* 1971;35(2):171–205. <https://doi.org/10.1128/br.35.2.171-205.1971>.
 44. Hutchens JO, Kass BM. A colorimetric microanalytical method for acetate and fluoroacetate. *J Biol Chem.* 1949;177(2):571–5. [https://doi.org/10.1016/S0021-9258\(18\)57000-9](https://doi.org/10.1016/S0021-9258(18)57000-9).
 45. Moran R. Formulae for determination of chlorophyllous pigments extracted with N N-dimethylformamide. *Plant Physiol.* 1982;69(6):1376–81. <https://doi.org/10.1104/pp.69.6.1376>.
 46. Chamovitz D, Sandmann G, Hirschberg J. Molecular and biochemical characterization of herbicide-resistant mutants of cyanobacteria reveals that phytoene desaturation is a rate-limiting step in carotenoid biosynthesis. *J Biol Chem.* 1993;268(23):17348–53.
 47. Vidal R, Venegas-Calderón M. Simple, fast and accurate method for the determination of glycogen in the model unicellular cyanobacterium *Synechocystis* sp. PCC 6803. *J Microbiol Methods.* 2019;164:105686. <https://doi.org/10.1016/j.mimet.2019.105686>.
 48. Ernst A, Kirschenlohr H, Diez J, Böger P. Glycogen content and nitrogenase activity in *Anabaena variabilis*. *Arch Microbiol.* 1984;140:120–5. <https://doi.org/10.1007/BF00454913>.
 49. Flores ME, Galston AW. Analysis of polyamines in higher plants by high performance liquid chromatography. *Plant Physiol.* 1982;69(3):701–6. <https://doi.org/10.1104/pp.69.3.701>.
 50. Jantaro S, Mäenpää P, Mulo P, Incharoensakdi A. Content and biosynthesis of polyamines in salt and osmotically stressed cells of *Synechocystis* sp. PCC 6803. *FEMS Microbiol Lett.* 2003;228(1):129–35. [https://doi.org/10.1016/S0378-1097\(03\)00747-X](https://doi.org/10.1016/S0378-1097(03)00747-X).
 51. Henderson JW, Ricker RD, Bidlingmeyer BA, Woodward C. Rapid, accurate, sensitive, and reproducible HPLC analysis of amino acids. Agilent Technologies, Application Note, Publication No: 5980–1193.
 52. Herbert P, Barros P, Ratola N, Alves A. HPLC determination of amino acids in musts and port wine using OPA/FMOC derivatives. *Food Chem Toxicol.* 2000;65(7):1130–3. <https://doi.org/10.1111/j.1365-2621.2000.tb10251.x>.

Publisher's Note

Springer Nature remains neutral with regard to jurisdictional claims in published maps and institutional affiliations.